



HAL
open science

Thermostable HIV-1 group O reverse transcriptase variants with the same fidelity as murine leukaemia virus reverse transcriptase

Verónica Barrioluengo, Mar Álvarez, Daniela Barbieri, Luis Menéndez-Arias

► To cite this version:

Verónica Barrioluengo, Mar Álvarez, Daniela Barbieri, Luis Menéndez-Arias. Thermostable HIV-1 group O reverse transcriptase variants with the same fidelity as murine leukaemia virus reverse transcriptase. *Biochemical Journal*, 2011, 436 (3), pp.599-607. 10.1042/BJ20101852 . hal-00596267

HAL Id: hal-00596267

<https://hal.science/hal-00596267>

Submitted on 27 May 2011

HAL is a multi-disciplinary open access archive for the deposit and dissemination of scientific research documents, whether they are published or not. The documents may come from teaching and research institutions in France or abroad, or from public or private research centers.

L'archive ouverte pluridisciplinaire **HAL**, est destinée au dépôt et à la diffusion de documents scientifiques de niveau recherche, publiés ou non, émanant des établissements d'enseignement et de recherche français ou étrangers, des laboratoires publics ou privés.

**Thermostable HIV-1 group O reverse transcriptase variants
with the same fidelity as murine leukaemia virus
reverse transcriptase**

**Verónica Barrioluengo, Mar Álvarez,
Daniela Barbieri¹ and Luis Menéndez-Arias***

*Centro de Biología Molecular “Severo Ochoa” (Consejo Superior de Investigaciones
Científicas – Universidad Autónoma de Madrid), 28049 Madrid, Spain*

Running title: High-fidelity HIV-1 group O RTs

¹ *Present address: Department of Haematology and Oncological Sciences “L. e A. Serragnoli”,
Microbiology Section, University of Bologna, 40138 Bologna, Italy*

** To whom correspondence should be addressed. Tel.: +34 911964494; Fax: +34 911964420; E-mail:
lmenendez@cbm.uam.es*

Abbreviations used: MLV, murine leukaemia virus; PCR, polymerase chain reaction; RT, reverse
transcriptase; WT, wild-type

ABSTRACT

Wild-type human immunodeficiency virus type 1 (HIV-1) group O reverse transcriptase (RT) shows increased thermostability in comparison with HIV-1 group M subtype B RT and murine leukemia virus (MLV) RT. However, its utility in the amplification of RNA targets is limited by the reduced accuracy of lentiviral RTs *versus* oncoretroviral RTs (*i.e.*, MLV RT). The effects of mutations K65R, R78A and K65R/V75I on the fidelity of HIV-1 group O RTs were studied by using gel-based and M13mp2 *lacZ* forward mutation fidelity assays. Forward mutation assays demonstrated that mutant RTs K65R, R78A and K65R/V75I showed >9-fold increased accuracy in comparison with the wild-type enzyme, and were about two times more faithful than the MLV RT. Compared with MLV RT, all tested HIV-1 group O RT variants showed decreased frameshift fidelity. However, K65R RT showed a higher tendency to introduce one-nucleotide deletions in comparison with other HIV-1 group O RT variants. R78A had a destabilizing effect on the RT, either in the presence or absence of V75I. At temperatures above 52°C, K65R and K65R/V75I retained similar levels of DNA polymerase activity to the wild-type HIV-1 group O RT but were more efficient than HIV-1 group M subtype B and MLV RTs. K65R, K65R/V75I and R78A RTs showed decreased misinsertion and mispair extension fidelity in comparison with the wild-type enzyme for most base pairs studied. These assays revealed that nucleotide selection is mainly governed by k_{pol} in the case of K65R, while both k_{pol} and K_{d} affect nucleotide discrimination in the case of K65R/V75I.

Key words: HIV, reverse transcriptase, fidelity, nucleotide incorporation, DNA polymerase, mutation

INTRODUCTION

The human immunodeficiency virus type 1 (HIV-1) reverse transcriptase (RT) is the enzyme responsible for the conversion of the viral genomic RNA into integration-competent double-stranded DNA [1]. The HIV-1 RT is a heterodimeric enzyme composed of subunits of 66 and 51 kDa, designated as p66 and p51, respectively. It shares structural homology with other DNA polymerases, including common subdomains (*i.e.*, fingers, palm and thumb) that in p66 form the nucleic acid binding cleft. Aspartic acid residues 110, 185 and 186 define the RT DNA polymerase active site in the palm of p66, which also contains an RNase H domain located at its C-terminus [2].

Reverse transcription is error prone and contributes to the high genetic variability of HIV-1. Studies with purified HIV-1 RT have revealed an unusually high error rate while copying DNA or RNA templates (for reviews, see [3,4]). Although reported error rates for HIV-1 RT show relatively large variability, ranging from 6×10^{-5} to 6.7×10^{-4} , it is widely assumed that oncoretroviral RTs (*e.g.* murine leukaemia virus (MLV) RT or avian myeloblastosis virus RT) are about 10 to 15 times more faithful than lentiviral RTs, including the HIV-1 enzyme [5,6]. HIV-1 is characterized by its remarkable variability. HIV-1 variants are classified into four major phylogenetic groups, designated as M (main), O (outlier), N (non-M/non-O) and P [7,8]. There are at least nine genetically distinct subtypes (or clades) of HIV-1 group M. These are subtypes A, B, C, D, F, G, H, J and K. Subtype B has been the dominant form in Europe, the Americas, Japan and Australia, and therefore HIV-1 group M subtype B RTs have been widely used as reference in virological and biochemical studies (*e.g.* RTs from clones HXB2, BH10 or NL4-3).

Mutational studies with HIV-1 RT have shown that molecular determinants of nucleotide specificity and fidelity of DNA synthesis map within the p66 subunit, mostly at or in the vicinity of the dNTP binding site (reviewed in ref. 4). Several amino acid substitutions in the HIV-1 RT (group M subtype B) have been shown to increase its intrinsic fidelity, as determined with the M13mp2 *lacZ* α forward mutation assay [9]. Examples are F61A [10], K65R [11], L74V [11-13], V75I [14], D76V [15], R78A [16], V148I [17], Q151N [18,19], and M184I [13,20-22].

Group O HIV-1 RTs differ in about 21% of their amino acid sequence when compared with their homologous counterparts of subtype B, and contain amino acid substitutions that confer resistance to non-nucleoside RT inhibitors [23,24]. We have recently demonstrated that a wild-type (WT) HIV-1 group O RT variant (derived from the ESP49 clone) shows increased thermal stability in comparison with MLV RT and a prototypic HIV-1 group M subtype B RT (*i.e.*, derived from the BH10 strain), while showing higher efficiency in reverse transcription PCRs that included a cDNA synthesis step performed at a high temperature range (57 – 69°C) [25]. In forward mutation assays, the WT HIV-1 group O RT showed 2.5-fold increased accuracy in comparison with the WT BH10 RT, and substituting Ile75 for Val produced a small additional increase in fidelity [25]. Now, we have studied the effects of mutations K65R and R78A on the thermostability and fidelity of DNA synthesis of HIV-1 group O RTs in the presence or absence of V75I. K65R and R78A were chosen as mutations that produced large increases in the fidelity of HIV-1 group M subtype B RTs, while retaining significant DNA polymerase activity [11,16,26,27]. Our results show that mutations K65R and K65R/V75I do not affect the thermal stability of the enzyme, but increase its accuracy to similar levels as the MLV RT. Mechanistic insights into the role of both mutations in the fidelity of DNA synthesis were obtained from transient kinetic assays.

EXPERIMENTAL

Mutagenesis, expression and purification of recombinant RTs

Site-directed mutagenesis was carried out with the Quik-Change Site-Directed Mutagenesis kit (Stratagene) by following the manufacturer's instructions, and using the following mutagenic primers: 5'-CTTTGCTATAAAAAGGAAAGATAGTACTAAGTGG-3' and 5'-CCACTTAGTACTATCTTTCCTTTTATAGCAAAG-3' for K65R, 5'-GCTGGTAGACTTTGCGGAATTAACAAGAG-3' and 5'-CTCTTGTTTAATTCCGCAAAGTCTACCAGC-3' for R78A, and 5'-GCTGATAGACTTTGCGGAATTAACAAGAGAAC-3' and 5'-GTTCTCTTGTTTAATTCCGCAAAGTCTATCAGC-3' for the double-mutant V75I/R78A. The plasmid p66RTB(O_WT) was used as template in the mutagenesis reactions involving the specific primers for K65R, R78A and V75I/R78A [25]. The double-mutant K65R/V75I was obtained with the K65R mutagenic primers and the template p66RTB plasmid containing the DNA that encodes for the V75I mutant of HIV-1 group O RT [25]. After mutagenesis, the entire RT-coding regions were sequenced and, if correct, used for RT expression and purification.

Recombinant RTs were expressed and purified as previously described [25,28,29]. RTs were co-expressed with HIV-1 protease in *E. coli* XL1 Blue to obtain p66/p51 heterodimers, which were later purified by ionic exchange followed by affinity chromatography. Purity of the enzymes was assessed by SDS-polyacrylamide gel electrophoresis. Enzymes were quantified by active site titration before biochemical studies [30]. The MLV RT was obtained from Promega.

DNA polymerase activity assays

Assays were carried out in 50 mM Tris-HCl (pH 8.0), 20 mM NaCl, 10 mM MgCl₂, 8 mM dithiothreitol, 50 μM [³H]dTTP (6-8 μCi/ml; 120-160 Ci/mol) (Perkin Elmer), and 1 μM template-primer (poly(rA)/oligo(dT)₁₆) (concentration expressed as 3'-hydroxyl primer termini) [25,31]. The thermal stability of RTs was determined by measuring the residual RNA-dependent DNA polymerase activity, after preincubating 60 μl of buffer containing the enzyme and the template-primer for 5 min at different temperatures in the range 37-60°C. For RT concentrations above 25 nM, preincubating the enzymes with the homopolymeric template-primer for up to 5 min at 37°C had a minor effect on their specific DNA polymerase activity. Polymerization reactions were initiated by adding 30 μl of buffer containing [³H]dTTP. The final active RT concentrations in these assays were around 20 nM. At different times, aliquots (20 μl) were removed into 20 μl of 0.5 M EDTA, and processed as previously described [31].

Reverse transcription PCR (RT-PCR) assays

The effect of the temperature on the efficiency of the reverse transcription reaction catalyzed by different RTs was determined by using a previously described two-step RT-PCR assay [25]. DNA amplifications were carried out with the Expand High Fidelity DNA polymerase mix (Roche). PCR primers used in these assays were: 5'-CCTAGGCACCAGGGTGTGAT-3' (ACT1), 5'-CGTACTCCTGCTTGCTGATCC-3' (ACT3), 5'-CTTCAGTGAGACAGGAGCTG-3' (TUB1), and 5'-CCACAGAATCCACACCAACC-3' (TUB2).

Pre-steady-state kinetic assays

Kinetic parameters for the incorporation of correct or incorrect nucleotides were determined as previously described [14,25], using 5'-³²P-labeled 21P (5'-ATACTTTAACCATATGTATCC-3') and 31T (5'-TTTTTTTTTAGGATACATATGGTTAAAGTAT-3'), as primer and template, respectively. Three additional primers (21PT, 21PG and 21PA) that differ from 21P in having T, G or A (instead of C) at their 3' terminus were used in mispair extension fidelity assays. Reactions were performed under single turnover conditions in a solution containing 50-100 nM (active sites) HIV-1 RT and a 100 nM concentration of template-primer 31T/21P, in RT buffer (50 mM Tris-HCl (pH 8.0), 50 mM KCl, 12-24 mM MgCl₂) and a variable concentration of nucleotide. Reactions involving the incorporation of incorrect nucleotides or mispair extension kinetics (i.e. incorporation of dCTP, dGTP or dATP on 31T/21P, or the extension of G:T, G:G and G:A mispairs) were conducted with excess concentration of the enzyme (120 nM) over the template-primer duplex (100 nM). These conditions were chosen to eliminate the influence of the enzyme turnover rate (k_{ss}), which interferes in the measurements of low incorporation rates.

M13mp2 *lacZa* forward mutation assays

Gapped duplex M13mp2 DNA was prepared as described previously [9], and used as template-primer for DNA synthesis reactions using purified WT or mutant RTs. Gap-filling synthesis reactions were performed in a 10- μ l reaction volume, containing 25 mM Tris-HCl (pH 8.0) buffer, 100 mM KCl, 2 mM dithiothreitol, 4 mM MgCl₂, 250 μ M of each dNTP (dATP, dGTP, dCTP and dTTP), 5 μ g/ml gapped duplex DNA and 100 nM RT [25]. The reactions were incubated at 37°C for 30 min and then stopped by adding 1 μ l of 60 mM EDTA.

Polymerization products were electroporated into *E. coli* MC1061 host cells, and after a brief (10-min) recovery period, transformants were plated on a bacterial indicator lawn (*E. coli* CSH50) in M9 plates containing 0.195 mM 5-bromo-4-chloro-3-indolyl- β -D-galactopyranoside and 0.2 mM isopropyl-1-thio- β -D-galactopyranoside. Mutant plaques were picked, their phenotype confirmed and the phage replicative form DNA isolated for nucleotide sequencing, using primer 5'-GCTTGCTGCAACTCTCTCAG-3' (Macrogen Inc., Seoul, South Korea).

Error frequencies were calculated as previously described [9]. At least ten fill-in reactions were performed for each enzyme. The nucleotide sequence of the entire gap region was determined for all mutant plaques. Specific error rates were derived by multiplying the corrected overall error frequency with the percentage of all mutations represented by the particular class of mutations (e.g., base substitutions). This number is divided by 0.6 (the average probability of an error being expressed in the M13mp2 assay) [6], and by the total number of sites where this class of mutations can be detected (e.g., 125 for base substitutions, and 148 for frameshifts).

RESULTS

Thermal stability of RTs

The residual RNA-dependent DNA polymerase activity of WT and mutant RTs obtained after preincubating the enzymes for 5 min at different temperatures, was determined in the presence of template-primer (i.e. poly(rA)/oligo(dT)₁₆). As shown in Figure 1, all tested enzymes showed similar amounts of residual activity after preincubations carried out at 42 to 48°C. However, the MLV RT and the mutant O_R78A RT showed reduced DNA polymerase activity

when the preincubation temperature was fixed at 50°C. At higher temperatures (*e.g.*, 54°C), four HIV-1 group O RT derivatives (*e.g.*, O_WT, O_V75I, O_K65R and O_K65R/V75I) retained 25 – 35% of their activity at 37°C, while the residual activities of BH10_WT and MLV RTs remained below 6% and 3%, respectively. Other HIV-1 group O RT variants such as O_R78A and the double-mutant O_V75I/R78A were found to be less stable than the BH10_WT RT. These mutant enzymes showed poor nucleotide incorporation efficiency at 37°C, and their specific activities were the lowest among all of the tested RTs (Figure 1, legend). Although the differences were relatively small, RT variants O_WT, O_K65R and O_K65R/V75I seem to be slightly more stable than the O_V75I RT as demonstrated by the results obtained after preincubating the RTs and the template-primer at 56°C.

The efficiency of reverse transcription at different temperatures was determined with a two-step RT-PCR assay including an initial cDNA synthesis reaction at a fixed temperature. The amplification of a 0.9-kb fragment of actin from mouse liver total RNA confirmed the reduced activity of the double-mutant O_V75I/R78A RT in assays including a reverse transcription step at 42°C (Figure 2A). In addition, this mutant showed no activity when the reverse transcription reactions were carried out at temperatures above 52°C. Both O_V75I/R78A and O_R78A RTs showed a low RT-PCR efficiency in comparison with the other HIV-1 RTs. These results were confirmed by the amplification of tubulin transcripts of 1.2 kb (Figure 2B). In these assays, MLV RT performed slightly better than both mutants at 57°C. Although most of the RTs were able to produce cDNA in the presence of a small amount of RNA (typically 10 to 50 ng), RNA inputs as high as 1 µg were required for efficient amplification of actin RNA in O_V75I/R78A RT-catalyzed reactions (Supplementary Figure S1). In contrast, WT HIV-1 group O RT and its mutants K65R and K65R/V75I retained significant activity at temperatures as high as 68°C in actin RNA amplifications, and also showed a better performance than the other RTs in tubulin RNA amplifications obtained after a reverse transcription step at 60°C.

Pre-steady-state kinetic analysis of thermostable HIV-1 group O RTs

Misinsertion and mispair extension fidelity assays were used to estimate the accuracy of DNA synthesis catalyzed by HIV-1 group O RTs. The kinetic parameters (k_{pol} and K_{d}) for the incorporation of correct (dTTP) and incorrect nucleotides (dCTP, dGTP or dATP) are given in Table 1. For dTTP incorporation, the catalytic efficiencies ($k_{\text{pol}}/K_{\text{d}}$) of studied RTs were in the range of $0.55 \mu\text{M}^{-1}\cdot\text{s}^{-1}$ to $1.82 \mu\text{M}^{-1}\cdot\text{s}^{-1}$, with O_R78A RT showing the lowest values. However, the $k_{\text{pol}}/K_{\text{d}}$ values for the incorporation of C, G or A by mutant O_K65R and O_K65R/V75I RTs were largely reduced.

The double-mutant K65R/V75I showed the highest misinsertion fidelities for the incorporation of A or C opposite A, although the differences with the single-mutant K65R were relatively small (Table 1; Supplementary Figure S2 A). The kinetic analysis showed that K65R produces a larger reduction of the k_{pol} for the incorporation of incorrect dNTPs in comparison with V75I. In comparison with the WT enzyme, the mutant O_R78A RT showed similar misinsertion fidelity for the incorporation of G or A opposite A, but increased efficiency of discrimination against C opposite A.

The kinetics of mispair extension were determined by measuring the incorporation of a correct T opposite A at the 3' end of the primer, using template-primer duplexes containing matched (G:C) or mismatched (G:T, G:G or G:A) termini. The results are shown in Table 2. Mismatched extension ratios were in the range of $0.24 - 2.3 \times 10^{-3}$ for the G:T mispair, $0.18 - 3.95 \times 10^{-4}$ for the G:G mispair, and lower than 2.2×10^{-6} for the G:A mispair. By themselves, mutations K65R and V75I produce a moderate increase in mispair extension fidelity, by

rendering enzymes with 2.8- to 5.4-fold decreased mismatched extension ratios (Table 2; Supplementary Figure S2 B). However, the double-mutant (O_K65R/V75I) showed 9.5- and 22.3-fold increases in mispair extension fidelity for G:T and G:G mismatches, respectively, suggesting an additive effect of both mutations. In the case of G:T mismatches, the increased mispair extension fidelity of O_K65R/V75I RT can be attributed to a loss in nucleotide binding affinity (K_d effect). However, in the case of G:G, the effects are due to the k_{pol} reduction observed for the incorporation of T on the mismatched template-primer. Interestingly, the single-mutant O_R78A RT was also highly accurate in mispair extension assays carried out with template-primers bearing G:T or G:G mismatches. As in the case of the O_K65R/V75I RT, discrimination efficiencies for G:T and G:G mispair extensions resulted from K_d - and k_{pol} -effects, respectively.

M13mp2 *lacZa* forward mutation assays

An M13mp2-based forward mutation assay was used to analyze how amino acid substitutions in the HIV-1 group O RT could affect its intrinsic fidelity. Mutations generated when the RT copies the gapped region of the *lacZ* gene in M13mp2 can be scored by the number of plaques with altered color phenotype (pale blue or colorless) in a specific indicator strain. Silent mutations are not detected in this assay. However, M13mp2 *lacZa* forward mutation assays provide a fidelity assessment based on a relatively large number of mutational target sites [9]. In these assays, mutant RTs O_K65R, O_K65R/V75I and O_R78A were >9 times more faithful than the WT HIV-1 group O enzyme (Table 3). Moreover, their mutant frequencies were 1.5 to 2.3 times lower than those calculated for the MLV RT. Although V75I confers 1.7-fold increased fidelity when introduced in a WT HIV-1 group O RT sequence context, this amino acid substitution had no effect on the RT's accuracy when the K65R mutation was present.

The mutational specificity of HIV-1 group O RTs bearing the amino acid substitutions K65R, K65R/V75I and R78A was determined after sequencing the *lacZa* mutants generated in the forward mutation assays. Their mutational spectra (Supplementary Figures S3, S4 and S5) were compared with those obtained with WT HIV-1 group O RT and mutant V75I [25] as well as with the MLV RT (Supplementary Figure S6). Unlike in the case of O_WT RT and mutant O_V75I RT, mutations generated by O_K65R, O_K65R/V75I and O_R78A RTs appear to be scattered throughout the target *lacZa* sequence. A mutational hot spot located next to runs of Ts at positions -36 to -34, and involving mostly T→C substitutions was observed with mutant RTs O_K65R/V75I and O_R78A. The O_K65R RT showed different mutational hot spots, located at positions -66 (G→T substitutions), +148 (one-nucleotide deletions or G→T substitutions), and +151 (mostly G→C substitutions). Unlike in the case of the WT enzyme (O_WT RT), frameshift errors represented 15.7 to 34.3% of all errors, in the mutational spectra generated by mutants K65R, K65R/V75I and R78A (Table 4). However, MLV RT had a higher propensity to introduce frameshift mutations, and showed frameshift error rates that were 3.5 to 11 times higher than those calculated for the three mutant HIV-1 group O RTs. These enzymes showed a remarkable tendency to generate one-nucleotide deletions, which in the case of the single-mutants K65R and R78A were predominantly located at non-runs. In addition, mutant O_K65R RT and in a lesser extent O_R78A RT showed a stronger tendency to generate transversions instead of transitions, a property shared by the MLV RT.

DISCUSSION

Mutational studies carried out with HIV-1 group M subtype B RTs allowed the identification of amino acid substitutions that produce significant increases in fidelity of DNA synthesis [10-22]. However, most of those amino acid changes have a negative effect on the specific DNA polymerase activity. Thus, substituting Ala for Phe61 produces an 11.7-fold increase in fidelity [10], while decreasing strand displacement DNA synthesis, processivity and template-primer binding [32,33]. On the other hand, mutant RTs with the amino acid substitutions V148I or Q151N showed 8.7- to 13.1-fold increased accuracy in comparison with the WT enzyme, although their catalytic efficiencies of dNTP incorporation were >23 times lower, as determined by using pre-steady-state kinetics [17,19]. Interestingly, K65R, V75I and R78A were previously identified as mutations that increased fidelity without impairing the DNA polymerase activity of HIV-1_{BH10} RT [11,14,16]. HIV-1_{NL4-3} mutant frequencies were also reduced when two of those mutations (*i.e.*, K65R and R78A) were introduced in the viral RT-coding region [34].

The interactions between the side-chain of Lys65 and the γ phosphate of the dNTP are important for the stabilization of the incoming nucleotide in the RT active site [35] (Figure 3). K65R confers resistance to dideoxynucleotide RT inhibitors and tenofovir, and this has been related to a reduction in the insertion rate (k_{pol}) of the nucleotide analogue [26,36,37; reviewed in ref. 38]. In addition, biochemical studies carried out with the HIV-1_{HXB2} RT demonstrated that K65R decreases mispair extension efficiency by reducing the catalytic rate of incorporation (k_{pol}) of correct dNTPs on mismatched template-primers [39]. These effects have been attributed in part to an incorrect positioning of the 3' end of the mispaired primer relative to the dNTP binding site [39]. Our results obtained with HIV-1 group O RTs are consistent with the previously observed k_{pol} -effect. However, we have also observed a significant reduction (4- to 8-fold decrease) in nucleotide misinsertion efficiencies when the K65R substitution was present. The k_{pol} reduction produced by K65R could be a consequence of the structural constraint imposed on Arg72, a residue that interacts with the β phosphate of the incoming dNTP, due to the formation of a stacking interaction between the guanidinium planes of Arg65 and Arg72 [40]. K65R exerts similar effects on the accuracy of HIV-1 group M subtype B and group O RTs, as determined in forward mutation assays [11]. Furthermore, with both types of RTs, the K65R mutation produces a higher ratio of transversions *versus* transitions and significant alterations in the mutational spectra. However, the K65R mutant displays increased frameshift fidelity over the WT HIV-1_{HXB2} RT, with a strong propensity to introduce deletions at nucleotide runs [11]. In contrast, the O_K65R RT shows a higher proportion of frameshift errors compared with the WT enzyme and a marked tendency to generate one-nucleotide deletions at non-runs.

Val75 and Arg78 are located at the base of the β 3- β 4 hairpin loop (residues 56-77), a site containing several residues involved in interactions with the incoming dNTP, that are important for drug resistance and fidelity of DNA synthesis [35; reviewed in ref. 38]. Both amino acids in the 66-kDa subunit of HIV-1 RT interact with the template nucleotide at position +1 (Figure 3). We have previously demonstrated that V75I produces a relatively modest increase in fidelity when introduced in HIV-1 RTs of groups M and O [14,25]. The mutational spectrum of the O_V75I RT was similar to that obtained with the WT enzyme [25]. Available evidence indicates that when introduced in HIV-1_{BH10} RT, R78A produces a large increase of fidelity as determined in forward mutation assays [16], but no information related to its mutational spectrum has been reported. Interestingly, the mutational spectrum of O_R78A RT shared with those of WT and mutant O_V75I RTs similar hot spot distributions (including a major hot spot at positions -34 to -36), very similar ratios of transitions *versus* transversions, and very low frameshift error rates. The types and frequencies of mutations generated by the

O_R78A RT were different from those obtained with the O_K65R RT that also showed a higher frameshift error rate than the O_R78A, O_V75I and WT RTs. The high fidelity of O_R78A RT is further confirmed by the results of our kinetic assays. This enzyme appears to be very inefficient in misincorporating C opposite A, as well as in extending G:T and G:G mispairs. Significant differences in the misincorporation ratios of A opposite A and G:T and G:A mispair extension efficiencies were found between O_K65R and O_R78A RTs. These results could justify in part the different mutational spectra obtained with both enzymes.

Substituting Ala for Arg78 has a destabilizing effect on the RT. The large effects on thermal stability observed with mutants R78A and V75I/R78A could be the result of the loss of interactions (mostly, hydrogen bonds) between the side chains of Arg78 and Asp76 that could affect the stability of the RT subunits. The specific RNA-dependent DNA polymerase activity at 37°C of the double-mutant (O_V75I/R78A RT) was about 3 times lower than the activity shown the WT enzyme. Both O_R78A and O_V75I/R78A showed largely reduced efficiency in RT-PCR reactions carried out at temperatures above 52°C, limiting their further development as high-fidelity thermostable RTs. V75I produced a small but detectable reduction in reverse transcription efficiency at high temperatures [25], when K65R was present, these effects were almost undetectable.

Mutants K65R and K65R/V75I showed similar accuracy in M13mp2 *lacZα* forward mutation assays. However, the observed mutational spectra were different. O_K65R RT showed a stronger tendency to generate frameshifts and produced more transversions than transitions. However, error specificities changed when V75I was present. Thus, the double-mutant showed a mutational spectrum with the hot spots at positions -34 to -36 and +87 found with O_V75I RT [25], but absent from the mutational spectrum of O_K65R RT. In addition, the double mutant showed a stronger tendency to generate one-nucleotide deletions at nucleotide runs, in comparison with the O_K65R RT. These results argue in favour of a functional interaction (or epistatic effect) between K65R and V75I, and against a dominant effect of any of both mutations.

Further evidence of this interaction has been obtained from gel-based fidelity assays. Previous kinetic studies showed that O_V75I RT increases both misinsertion and mispair extension fidelity [14,25]. Unlike in the case of O_K65R RT, nucleotide affinity loss (*i.e.*, increased K_d for nucleotide incorporation on mismatched template-primers) had a significant effect on the reduced mispair extension efficiencies of O_V75I RT. The double mutant K65R/V75I showed increased mispair extension fidelity for G:T and G:G mismatches, in comparison with the single mutants K65R and V75I. The increased accuracy of the double mutant was largely dominated by a K_d effect in the case of G:T mispair extension, while in the case of G:G mispairs both k_{pol} and K_d values were affected by the presence of K65R together with V75I. Interestingly, these effects on G:T and G:G mispair extension were also observed with the R78A mutant. Interactions between the tip of the β 3- β 4 hairpin loop (including Lys65) and the dNTP could be largely affected by removal of the side-chain of Arg78 that could have a strong influence on the conformation of the β 3- β 4 hairpin loop and its interactions with template nucleotide at position +1.

In summary, we provide evidence that demonstrates that the fidelity of lentiviral RTs (*i.e.*, HIV-1 RT) can be improved to the levels shown by the more faithful murine leukaemia virus RT, without altering the stability or the specific DNA polymerase activity of the enzyme. O_K65R, O_K65R/V75I and O_R78A RTs showed >10-fold increased accuracy for base substitutions in comparison with the WT enzyme. Base substitution error rates were similar to those obtained with MLV RT. However, the MLV RT showed a higher error rate for frameshifts (*e.g.*, >3 times higher than for K65R) and a stronger tendency to produce

transversions *versus* transitions in forward mutation assays. Overall error rates for MLV RT are also in good agreement with previous estimates obtained with the M13mp2 *lacZ* α forward mutation assay [5,6]. However, pre-steady-state kinetics analyses of fidelity using MLV RT were limited by its low catalytic efficiency in comparison with HIV-1 RTs [41; data not shown], as well as by the requirement of high concentrations of enzyme. The higher fidelity of the MLV RT in comparison with HIV-1 RT has been previously shown in gel-based assays using synthetic heteropolymeric template-primers [41-44]. Most of those studies have been carried out under steady-state conditions. Reported misinsertion and mispair extension ratios for MLV RT were about 2 to 8 times lower than those obtained with HIV-1 RT [42-44]. However, results were strongly dependent on the sequence and the template-primer used. Therefore, in this scenario, forward mutation assays provide a more reliable estimate of fidelity differences between both enzymes.

Although the role of K65R in the acquisition of drug resistance in HIV-1 group O RT has not been studied in detail in the clinical setting, a recent report estimates that about 10% of the HIV-1 (group M subtype B) clinical isolates bearing the K65R mutation also contain V75I [45]. It remains to be determined whether the RTs found *in vivo* display high fidelity and if this property has any impact on viral evolution. In any case, the RTs described in this work combine increased efficiency of reverse transcription at high temperatures with high fidelity, and should be of great utility in the amplification of RNA targets.

ACKNOWLEDGMENTS

We thank Dr. Thomas Kunkel for helpful advice.

FUNDING

This work was supported by grants of the Ministry of Science and Innovation of Spain (BIO2007/60319 and BIO2010/15542), Fundación para la Investigación y Prevención del SIDA en España (FIPSE) (grant 36771/08), Fondo de Investigación Sanitaria (through the “Red Temática de Investigación Cooperativa en SIDA” RD06/006), and an institutional grant from the Fundación Ramón Areces.

REFERENCES

1. Herschhorn, A. and Hizi, A. (2010) Retroviral reverse transcriptases. *Cell. Mol. Life Sci.*, **67**, 2717–2747
2. Sarafianos, S. G., Marchand, B., Das, K., Himmel, D. M., Parniak, M. A., Hughes, S. H. and Arnold, E. (2009) Structure and function of HIV-1 reverse transcriptase: Molecular mechanisms of polymerization and inhibition. *J. Mol. Biol.*, **385**, 693–713
3. Menéndez-Arias, L. (2002) Molecular basis of DNA synthesis and nucleotide specificity of retroviral reverse transcriptases. *Prog. Nucleic Acids Res. Mol. Biol.*, **71**, 91–147
4. Menéndez-Arias, L. (2009) Mutation rates and intrinsic fidelity of retroviral reverse transcriptases. *Viruses (Basel)*, **1**, 1137-1165
5. Roberts, J. D., Bebenek, K. and Kunkel, T. A. (1988) The accuracy of reverse transcriptase from HIV-1. *Science*, **242**, 1171–1173.

6. Roberts, J. D., Preston, B. D., Johnston, L. A., Soni, A., Loeb, L. A. and Kunkel, T. A. (1989) Fidelity of two retroviral reverse transcriptases during DNA-dependent DNA synthesis in vitro. *Mol. Cell. Biol.*, **9**, 469–476
7. Buonaguro, L., Tornesello, M. L. and Buonaguro, F. N. (2007) Human immunodeficiency virus type 1 subtype distribution in the worldwide epidemic: pathogenic and therapeutic implications. *J. Virol.*, **81**, 10209–10219
8. Plantier, J. C., Leoz, M., Dickerson, J. E., De Oliveira, F., Cordonnier, F., Lemée, V., Damond, F., Robertson, D. L. and Simon, F. (2009) A new human immunodeficiency virus derived from gorillas. *Nat. Med.*, **15**, 871–872
9. Bebenek, K. and Kunkel, T. A. (1995) Analyzing fidelity of DNA polymerases. *Methods Enzymol.*, **262**, 217–232
10. Fisher, T. S. and Prasad, V. R. (2002) Substitutions of Phe⁶¹ located in the vicinity of template 5'-overhang influence polymerase fidelity and nucleoside analog sensitivity of HIV-1 reverse transcriptase. *J. Biol. Chem.*, **277**, 22345–22352
11. Shah, F. S., Curr, K. A., Hamburgh, M. E., Parniak, M., Mitsuya, H., Arnez, J. G. and Prasad, V. R. (2000) Differential influence of nucleoside analog-resistance mutations K65R and L74V on the overall mutation rate and error specificity of human immunodeficiency virus type 1 reverse transcriptase. *J. Biol. Chem.*, **275**, 27037–27044
12. Rubinek, T., Bakhanashvili, M., Taube, R., Avidan, O. and Hizi, A. (1997) The fidelity of 3' misinsertion and mispair extension during DNA synthesis exhibited by two drug-resistant mutants of the reverse transcriptase of human immunodeficiency virus type 1 with Leu74→Val and Glu89→Gly. *Eur. J. Biochem.*, **247**, 238–247
13. Jonckheere, H., De Clercq, E. and Anné, J. (2000) Fidelity analysis of HIV-1 reverse transcriptase mutants with an altered amino-acid sequence at residues Leu74, Glu89, Tyr115, Tyr183 and Met184. *Eur. J. Biochem.*, **267**, 2658–2665
14. Matamoros, T., Kim, B. and Menéndez-Arias, L. (2008) Mechanistic insights into the role of Val75 of HIV-1 reverse transcriptase in misinsertion and mispair extension fidelity of DNA synthesis. *J. Mol. Biol.*, **375**, 1234–1248
15. Kim, B., Hathaway, T. R. and Loeb, L. A. (1998) Fidelity of mutant HIV-1 reverse transcriptases: interaction with the single-stranded template influences the accuracy of DNA synthesis. *Biochemistry*, **37**, 5831–5839
16. Kim, B., Ayran, J. C., Sagar, S. G., Adman, E. T., Fuller, S. M., Tran, N. H. and Horrigan, J. (1999) New human immunodeficiency virus type 1 reverse transcriptase (HIV-1 RT) mutants with increased fidelity of DNA synthesis. *J. Biol. Chem.*, **274**, 27666–27673
17. Weiss, K. K., Chen, R., Skasko, M., Reynolds, H. M., Lee, K., Bambara, R. A., Mansky, L. M. and Kim, B. (2004) A role for dNTP binding of human immunodeficiency virus type 1 reverse transcriptase in viral mutagenesis. *Biochemistry*, **43**, 4490–4500
18. Weiss, K. K., Isaacs, S. J., Tran, N. H., Adman, E. T. and Kim, B. (2000) Molecular architecture of the mutagenic active site of human immunodeficiency virus type 1 reverse transcriptase: roles of the β8-αE loop in fidelity, processivity, and substrate interactions. *Biochemistry*, **39**, 10684–10694
19. Weiss, K. K., Bambara, R. A., Kim, B. (2002) Mechanistic role of residue Gln¹⁵¹ in error prone DNA synthesis by human immunodeficiency virus type 1 (HIV-1) reverse transcriptase (RT). Pre-steady state kinetic study of the Q151N HIV-1 RT mutant with increased fidelity. *J. Biol. Chem.*, **277**, 22662–22669

20. Hsu, M., Inouye, P., Rezende, L., Richard, N., Li, Z., Prasad, V. R. and Wainberg, M. A. (1997) Higher fidelity of RNA-dependent DNA mispair extension by M184V drug-resistant than wild-type reverse transcriptase of human immunodeficiency virus type 1. *Nucleic Acids Res.*, **25**, 4532–4536
21. Oude Essink, B. B., Back, N. K. T. and Berkhout, B. (1997) Increased polymerase fidelity of the 3TC-resistant variants of HIV-1 reverse transcriptase. *Nucleic Acids Res.*, **25**, 3212–3217
22. Rezende, L. F., Drosopoulos, W. C. and Prasad, V. R. (1998) The influence of 3TC resistance mutation M184I on the fidelity and error specificity of human immunodeficiency virus type 1 reverse transcriptase. *Nucleic Acids Res.*, **26**, 3066–3072
23. Quiñones-Mateu, M. E., Soriano, V., Domingo, E. and Menéndez-Arias, L. (1997) Characterization of the reverse transcriptase of a human immunodeficiency virus type 1 group O isolate. *Virology*, **236**, 364–373
24. Menéndez-Arias, L., Abraha, A., Quiñones-Mateu, M. E., Mas, A., Camarasa, M.-J. and Arts, E. J. (2001) Functional characterization of chimeric reverse transcriptases with polypeptide subunits of highly divergent HIV-1 group M and O strains. *J. Biol. Chem.*, **276**, 27470–27479
25. Álvarez, M., Matamoros, T. and Menéndez-Arias, L. (2009) Increased thermostability and fidelity of DNA synthesis of wild-type and mutant HIV-1 group O reverse transcriptases. *J. Mol. Biol.*, **392**, 872–884
26. Sluis-Cremer, N., Arion, D., Kaushik, N., Lim, H. and Parniak, M. A. (2000) Mutational analysis of Lys⁶⁵ of HIV-1 reverse transcriptase. *Biochem. J.*, **348**, 77–82
27. Garforth, S. J., Kim, T. W., Parniak, M. A., Kool, E. T. and Prasad, V. R. (2007) Site-directed mutagenesis in the fingers subdomain of HIV-1 reverse transcriptase reveals a specific role for the β 3- β 4 hairpin loop in dNTP selection. *J. Mol. Biol.*, **365**, 38–49
28. Boretto, J., Longhi, S., Navarro, J.-M., Selmi, B., Sire, J. and Canard, B. (2001) An integrated system to study multiply substituted human immunodeficiency virus type 1 reverse transcriptase. *Anal. Biochem.*, **292**, 139–147
29. Matamoros, T., Deval, J., Guerreiro, C., Mulard, L., Canard, B. and Menéndez-Arias, L. (2005) Suppression of multidrug-resistant HIV-1 reverse transcriptase primer unblocking activity by α -phosphate-modified thymidine analogues. *J. Mol. Biol.*, **349**, 451–463
30. Kati, W. M., Johnson, K. A., Jerva, L. F. and Anderson, K. S. (1992) Mechanism and fidelity of HIV reverse transcriptase. *J. Biol. Chem.*, **267**, 25988–25997
31. Martín-Hernández, A. M., Gutiérrez-Rivas, M., Domingo, E. and Menéndez-Arias, L. (1997) Mismatch extension fidelity of human immunodeficiency virus type 1 reverse transcriptases with amino acid substitutions affecting Tyr115. *Nucleic Acids Res.*, **25**, 1383–1389
32. Mandal, D., Dash, C., Le Grice, S. F. J. and Prasad, V. R. (2006) Analysis of HIV-1 replication block due to substitutions at F61 residue of reverse transcriptase reveals additional defects involving the RNase H function. *Nucleic Acids Res.*, **34**, 2853–2863
33. Agopian, A., Depollier, J., Lionne, C. and Divita, G. (2007) p66 Trp24 and Phe61 are essential for accurate association of HIV-1 reverse transcriptase with primer/template. *J. Mol. Biol.*, **373**, 127–140

34. Mansky, L. M., Le Rouzic, E., Benichou, S. and Gajary, L. C. (2003) Influence of reverse transcriptase variants, drugs, and Vpr on human immunodeficiency virus type 1 mutant frequencies. *J. Virol.*, **77**, 2071–2080
35. Huang, H., Chopra, R., Verdine, G. L. and Harrison, S. C. (1998) Structure of a covalently trapped catalytic complex of HIV-1 reverse transcriptase: implications for drug resistance. *Science*, **282**, 1669–1675
36. Deval, J., Navarro, J.-M., Selmi, B., Courcambeck, J., Boretto, J., Halfon, P., Garrido-Urbani, S., Sire, J. and Canard, B. (2004) A loss of viral replicative capacity correlates with altered DNA polymerization kinetics by the human immunodeficiency virus reverse transcriptase bearing the K65R and L74V dideoxynucleoside resistance substitutions. *J. Biol. Chem.*, **279**, 25489–25496
37. Sluis-Cremer, N., Sheen, C.-W., Zelina, S., Torres, P. S. A., Parikh, U. M. and Mellors, J. W. (2007) Molecular mechanism by which the K70E mutation in human immunodeficiency virus type 1 reverse transcriptase confers resistance to nucleoside reverse transcriptase inhibitors. *Antimicrob. Agents Chemother.*, **51**, 48–53
38. Menéndez-Arias, L. (2008) Mechanisms of resistance to nucleoside analogue inhibitors of HIV-1 reverse transcriptase. *Virus Res.*, **134**, 124–146
39. Garforth, S. J., Domaol, R. A., Lwatula, C., Landau, M. J., Meyer, A. J., Anderson, K. S. and Prasad, V. R. (2010) K65R and K65A substitutions in HIV-1 reverse transcriptase enhance polymerase fidelity by decreasing both dNTP misinsertion and mispaired primer extension efficiencies. *J. Mol. Biol.*, **401**, 33–44
40. Das, K., Bandwar, R. P., White, K. L., Feng, J. Y., Sarafianos, S. G., Tuske, S., Tu, X., Clark, A. D. Jr., Boyer, P. L., Hou, X., Gaffney, B. L., Jones, R. A., Miller, M. D., Hughes, S. H. and Arnold, E. (2009) Structural basis for the role of the K65R mutation in HIV-1 reverse transcriptase polymerization, excision antagonism, and tenofovir resistance. *J. Biol. Chem.*, **284**, 35092–35100
41. Skasko, M., Weiss, K. K., Reynolds, H. M., Jamburuthugoda, V., Lee, K. and Kim, B. (2005) Mechanistic differences in RNA-dependent DNA polymerization and fidelity between murine leukemia virus and HIV-1 reverse transcriptases. *J. Biol. Chem.*, **280**, 12190–12200
42. Ricchetti, M. and Buc, H. (1990) Reverse transcriptases and genomic variability: the accuracy of DNA replication is enzyme specific and sequence dependent. *EMBO J.*, **9**, 1583–1593
43. Bakhanashvili, M. and Hizi, A. (1992) Fidelity of the RNA-dependent DNA synthesis exhibited by the reverse transcriptases of human immunodeficiency virus types 1 and 2 and of murine leukemia virus: Mismatch extension frequencies. *Biochemistry*, **31**, 9393–9398
44. Bakhanashvili, M. and Hizi, A. (1993) The fidelity of the reverse transcriptases of human immunodeficiency viruses and murine leukemia virus, exhibited by the mismatch extension frequencies, is sequence dependent and enzyme related. *FEBS Lett.*, **319**, 201–205
45. McColl, D. J., Chappey, C., Parkin, N. T. and Miller, M. D. (2008) Prevalence, genotypic associations and phenotypic characterization of K65R, L74V and other HIV-1 RT resistance mutations in a commercial database. *Antivir. Ther.*, **13**, 189–197

LEGEND TO FIGURES

Figure 1. Thermal stability of RTs.

RNA-dependent DNA polymerization reactions were carried out at 37°C in the presence of 1 μ M poly(rA)/oligo(dT)₁₆ and 50 μ M [³H]dTTP. The active RT concentration in the assay was 15–20 nM. Relative dTTP incorporation rates were measured after preincubating the enzymes with the template/primer for 5 min at the indicated temperatures. For each enzyme, percent activity was normalized relative to the value obtained after preincubating the RTs at 37°C (100%). Reported values for each enzyme were obtained from at least four independent experiments. The nucleotide incorporation rates obtained after preincubating the enzymes at 37°C were $0.72 \pm 0.28 \text{ s}^{-1}$ for O_WT RT, $0.92 \pm 0.25 \text{ s}^{-1}$ for O_K65R RT, $0.61 \pm 0.26 \text{ s}^{-1}$ for O_K65R/V75I RT, $0.45 \pm 0.06 \text{ s}^{-1}$ for O_R78A RT, $0.25 \pm 0.06 \text{ s}^{-1}$ for O_V75I/R78A RT, $0.57 \pm 0.06 \text{ s}^{-1}$ for O_V75I RT, $1.17 \pm 0.4 \text{ s}^{-1}$ for BH10_WT RT, and $1.16 \pm 0.4 \text{ s}^{-1}$ for MLV RT.

Figure 2. Effect of temperature on cDNA synthesis and two-step RT-PCR.

The cDNA synthesis reactions were carried out for 60 min at the indicated temperatures, in a buffer containing 50 ng/ μ l of mouse liver RNA and 150 nM RT (active site concentration). Reactions were stopped by heating at 92°C for 10 min. Two microliters of the cDNA synthesis reaction and 1.75 units of Expand High Fidelity DNA polymerase mix were used in all amplifications. Panel A shows amplifications of a 0.9-Kb fragment of actin DNA, obtained with primers ACT1 and ACT3. Panel B shows amplifications of a 1.2-Kb fragment of tubulin DNA, obtained with primers TUB1 and TUB2. Lanes 1 and C show molecular weight markers (HindIII digest of phage Φ 29 DNA), and a control reaction (carried out in the absence of RT), respectively. Lanes 2 to 9 show the result of two-step RT-PCRs that included a cDNA synthesis step, carried out with O_K65R RT (lane 2), O_K65R/V75I RT (lane 3), O_R78A RT (lane 4), O_V75I/R78A RT (lane 5), O_WT RT (lane 6), O_V75I RT (lane 7), BH10_WT RT (lane 8) and MLV RT (lane 9). Data are representative of three independent experiments.

Figure 3. Crystal structures of the ternary complex of HIV-1 RT bound to double-stranded DNA (dsDNA) and dTTP showing the location of Lys65, Val75 and Arg78 in the 66-kDa subunit of the enzyme.

(A) Ternary complex of HIV-1 [group M subtype B (isolate HXB2)] RT, dsDNA and dTTP (PDB file 1RTD) [35]. The RT subunits p66 and p51 are represented by cyan and green ribbons, respectively. The template and primer strands are represented with grey and white sphere models. The incoming dNTP is shown in yellow. The side chains of Lys65, Val75 and Arg78 are shown in blue, magenta and orange, respectively. Panel (B) shows the β 3- β 4 hairpin loop and the dNTP binding site with the location of relevant residues.

Table 1. Pre-steady-state kinetic parameters for misincorporation

Enzyme	Nucleotide	k_{pol} (s^{-1})	K_{d} (μM)	$k_{\text{pol}}/K_{\text{d}}$ ($\mu\text{M}^{-1}\cdot\text{s}^{-1}$)	Misinsertion ratio (f_{ins}) ^a
O_WT RT ^b	dTTP	14.7 ± 1.0	11.8 ± 2.9	1.25 ± 0.32	
	dCTP	0.72 ± 0.10	7652 ± 2083	(9.5 ± 2.9) × 10 ⁻⁵	7.57 × 10 ⁻⁵
	dGTP	0.15 ± 0.03	11730 ± 3750	(1.3 ± 0.5) × 10 ⁻⁵	1.03 × 10 ⁻⁵
	dATP	(7.3 ± 0.2) × 10 ⁻³	1485 ± 150	(4.9 ± 2.2) × 10 ⁻⁶	3.94 × 10 ⁻⁶
O_V75I RT ^b	dTTP	13.9 ± 1.2	14.6 ± 4.3	0.96 ± 0.30	
	dCTP	0.27 ± 0.05	11023 ± 3792	(2.4 ± 0.9) × 10 ⁻⁵	2.54 × 10 ⁻⁵ (3.0)
	dGTP	(6.3 ± 0.9) × 10 ⁻²	7481 ± 2307	(8.4 ± 2.9) × 10 ⁻⁶	8.76 × 10 ⁻⁶ (1.2)
	dATP	(2.2 ± 0.2) × 10 ⁻³	2308 ± 720	(9.5 ± 3.1) × 10 ⁻⁷	9.98 × 10 ⁻⁷ (3.9)
O_K65R RT	dTTP	10.7 ± 0.9	5.8 ± 1.9	1.82 ± 0.60	
	dCTP	0.17 ± 0.02	9559 ± 1908	(1.7 ± 0.4) × 10 ⁻⁵	9.51 × 10 ⁻⁶ (8.0)
	dGTP	(3.1 ± 1.9) × 10 ⁻²	6452 ± 857	(4.8 ± 0.7) × 10 ⁻⁶	2.66 × 10 ⁻⁶ (3.9)
	dATP	(4.8 ± 0.1) × 10 ⁻³	3680 ± 178	(1.3 ± 0.1) × 10 ⁻⁶	7.09 × 10 ⁻⁷ (5.6)
O_K65R/V75I RT	dTTP	12.7 ± 1.3	13.3 ± 3.7	0.95 ± 0.28	
	dCTP	(3.3 ± 0.3) × 10 ⁻²	5686 ± 995	(5.8 ± 1.1) × 10 ⁻⁶	6.06 × 10 ⁻⁶ (12.5)
	dGTP	0.11 ± 0.02	13430 ± 4605	(8.3 ± 3.3) × 10 ⁻⁶	8.70 × 10 ⁻⁶ (1.2)
	dATP	(3.3 ± 0.2) × 10 ⁻³	5290 ± 553	(6.2 ± 0.7) × 10 ⁻⁷	6.52 × 10 ⁻⁷ (6.0)
O_R78A RT	dTTP	9.4 ± 1.1	17.2 ± 5.3	0.55 ± 0.18	
	dCTP	(1.6 ± 0.2) × 10 ⁻²	6939 ± 1740	(2.4 ± 0.7) × 10 ⁻⁶	4.27 × 10 ⁻⁶ (17.7)
	dGTP	(6.2 ± 0.4) × 10 ⁻³	2313 ± 361	(2.7 ± 0.5) × 10 ⁻⁶	4.89 × 10 ⁻⁶ (2.1)
	dATP	(1.9 ± 0.7) × 10 ⁻³	1122 ± 165	(1.7 ± 0.3) × 10 ⁻⁶	3.13 × 10 ⁻⁶ (1.4)

The template-primer 31T/21P was used as the substrate. Data shown are the mean values ± standard deviation. Each of the assays was performed independently at least three times.

^a $f_{\text{ins}} = [k_{\text{pol}}(\text{incorrect})/K_{\text{d}}(\text{incorrect})]/[k_{\text{pol}}(\text{correct})/K_{\text{d}}(\text{correct})]$, where incorrect nucleotides were dCTP, dGTP or dATP, while the correct nucleotide was dTTP. Numbers between parentheses represent the relative increase of fidelity, as determined for each incorrect nucleotide as the ratio: f_{ins} (O_WT RT) / f_{ins} (mutant RT).

^b Reported values for O_WT RT and O_V75I RT were taken from ref. [25].

Table 2. Pre-steady-state kinetic parameters for mispair extension

Enzyme	Base pair at the 3' end ^a	k_{pol} (s ⁻¹)	K_d (μM)	k_{pol}/K_d (μM ⁻¹ ·s ⁻¹)	Mismatch extension ratio (f_{ext}) ^b
O_WT RT ^c	G:C	14.7 ± 1.0	11.8 ± 2.9	1.25 ± 0.32	
	G:T	7.6 ± 0.9	2638 ± 785	(2.9 ± 0.9) × 10 ⁻³	2.30 × 10 ⁻³
	G:G	0.56 ± 0.07	1132 ± 316	(4.9 ± 1.5) × 10 ⁻⁴	3.95 × 10 ⁻⁴
	G:A	(2.1 ± 0.3) × 10 ⁻²	7817 ± 2334	(2.7 ± 0.9) × 10 ⁻⁶	2.17 × 10 ⁻⁶
O_V75I RT ^c	G:C	13.9 ± 1.2	14.6 ± 4.3	0.96 ± 0.30	
	G:T	2.8 ± 0.2	4400 ± 789	(6.3 ± 1.2) × 10 ⁻⁴	6.56 × 10 ⁻⁴ (3.5)
	G:G	0.32 ± 0.01	2426 ± 178	(1.3 ± 0.1) × 10 ⁻⁴	1.39 × 10 ⁻⁴ (2.8)
	G:A	(6.8 ± 0.8) × 10 ⁻³	12110 ± 2536	(5.6 ± 1.3) × 10 ⁻⁷	5.86 × 10 ⁻⁷ (3.7)
O_K65R RT	G:C	10.7 ± 0.9	5.8 ± 1.9	1.82 ± 0.60	
	G:T	3.1 ± 0.5	2214 ± 1058	(1.4 ± 0.7) × 10 ⁻³	7.80 × 10 ⁻⁴ (2.9)
	G:G	0.19 ± 0.02	1416 ± 328.4	(1.3 ± 0.3) × 10 ⁻⁴	7.25 × 10 ⁻⁵ (5.4)
	G:A	(1.3 ± 0.2) × 10 ⁻²	15180 ± 4239	(8.7 ± 2.9) × 10 ⁻⁷	4.78 × 10 ⁻⁷ (4.5)
O_K65R/V75I RT	G:C	12.7 ± 1.3	13.3 ± 3.7	0.95 ± 0.28	
	G:T	2.4 ± 0.2	10450 ± 1644	(2.3 ± 0.4) × 10 ⁻⁴	2.43 × 10 ⁻⁴ (9.5)
	G:G	(8.7 ± 0.9) × 10 ⁻²	5213 ± 1096	(1.7 ± 0.4) × 10 ⁻⁵	1.77 × 10 ⁻⁵ (22.3)
	G:A	(1.4 ± 0.1) × 10 ⁻³	3578 ± 786	(3.9 ± 0.9) × 10 ⁻⁷	4.15 × 10 ⁻⁷ (5.2)
O_R78A RT	G:C	9.4 ± 1.1	17.2 ± 5.3	0.55 ± 0.18	
	G:T	1.4 ± 0.2 ^d	>8000	ND	ND
	G:G	(3.4 ± 0.3) × 10 ⁻²	2158 ± 484	(1.6 ± 0.4) × 10 ⁻⁵	2.87 × 10 ⁻⁵ (13.8)
	G:A	(2.0 ± 0.2) × 10 ⁻³	2926 ± 572	(6.8 ± 1.4) × 10 ⁻⁷	1.24 × 10 ⁻⁶ (1.8)

The template-primer 31T/21P was used as the substrate. Data shown are the mean values ± standard deviation. Each of the assays was performed independently at least three times.

^a The first base corresponds to the template and the second to the primer.

^b $f_{\text{ext}} = [k_{\text{pol}}(\text{mismatched})/K_d(\text{mismatched})]/[k_{\text{pol}}(\text{matched})/K_d(\text{matched})]$. Numbers between parenthesis represent the relative increase of fidelity, as determined for each mispair as the ratio: $f_{\text{ext}}(\text{O_WT RT})/f_{\text{ext}}(\text{mutant RT})$.

^c Reported values for O_WT RT and O_V75I RT were taken from ref. [25].

^d A linear relationship between k_{obs} and [dTTP] was observed at nucleotide concentrations between 0.5 and 12 mM. The reported value is the k_{obs} obtained at 12 mM dTTP. ND, not determined.

Table 3. Accuracy of RT variants in M13mp2 *lacZ* forward mutation assays.

Enzymes	Total plaques	Mutant plaques	Mutant frequency ^a	Fidelity (fold change)	
				(relative to O_WT RT)	(relative to MLV RT)
O_WT RT ^b	7579	63	0.00831	1	0.16
O_K65R RT	75474	58	0.00077	10.8	1.8
O_K65R/V75I RT	55657	50	0.00089	9.3	1.5
O_V75I RT ^b	9894	47	0.00475	1.7	0.28
O_R78A RT	80664	48	0.00059	14.1	2.3
MLV RT	29648	40	0.00135	6.2	1

^a Reported background frequencies in this assay (usually around 6×10^{-4}) [9,14] are in most cases a consequence of M13mp2 DNA rearrangements that result in the loss of the *lacZ* gene. In order to have a better estimate of the background due to errors introduced by *E. coli* polymerases while copying the *lacZ* sequence, phage DNA was obtained from all mutant plaques and the sequence of the reporter gene was determined in all cases. In control experiments involving a total of 22189 plaques, no mutations in *lacZ* were identified after analyzing the results obtained from 2-3 *E. coli* electroporations carried out with gapped M13mp2 DNA substrate.

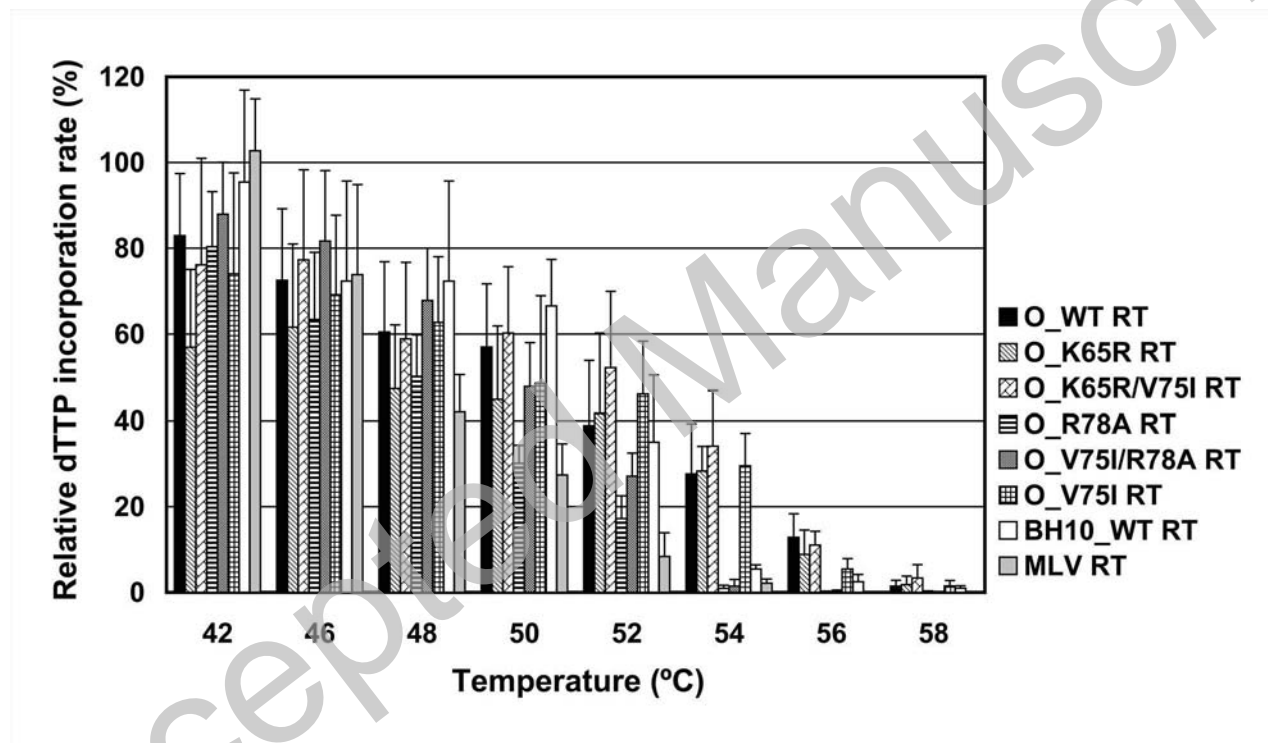
^b Reported values for O_WT RT and O_V75I RT were taken from ref. [25].

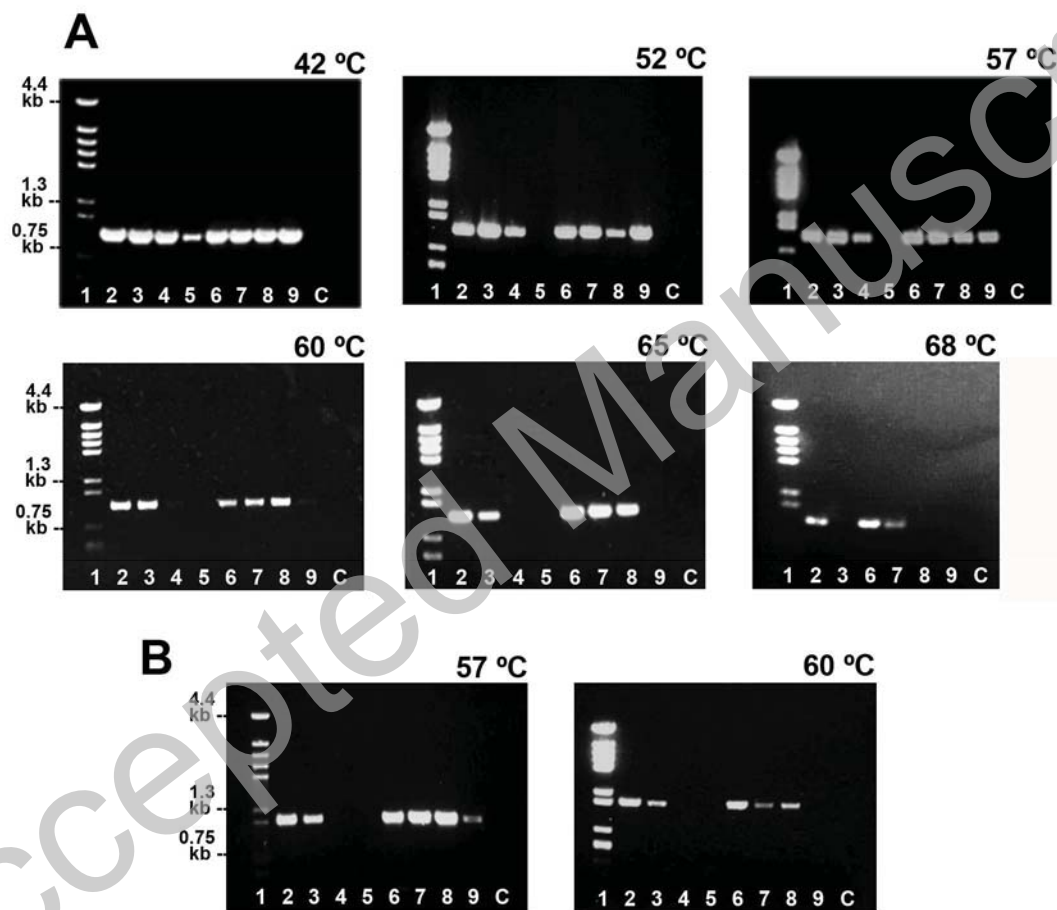
Table 4. Summary of error rates for RTs, for various classes of mutations.

Mutation type	O_WT RT ^a		O_K65R RT		O_K65R/V75I RT		O_R78A RT		MLV RT	
	No. of errors	Error rate	No. of errors	Error rate	No. of errors	Error rate	No. of errors	Error rate	No. of errors	Error rate
<i>All classes</i>	49	1/17166	67	1/160185 (9.3) ^b	50	1/158288 (9.2)	51	1/224910 (13.1)	49	1/86040 (5.0)
<i>Base substitutions</i>	49	1/9053	44	1/128649 (14.2)	39	1/107033 (11.8)	43	1/140693 (15.5)	19	1/117032 (12.9)
Transitions	25 (51%)		8 (18.2%)		21 (53.8%)		19 (44.2%)		3 (15.8%)	
Transversions	24 (49%)		36 (81.8%)		18 (46.2%)		24 (55.8%)		16 (84.2%)	
<i>Frameshifts</i>	0	<1/541516	23	1/291395 (<0.5)	11	1/449304 (<0.8)	8	1/895370 (<1.7)	30	1/87758 (<0.16)
Insertions	0		2 (8.7%)		1 (9.1%)		1 (12.5%)		8 (26.7%)	
Deletions	0		21 (91.3%)		10 (90.9%)		7 (87.5%)		22 (73.3%)	
At runs	0	<1/280371	6	1/596245 (<2.1)	6	1/439690 (<1.6)	2	1/1911737 (<6.8)	14	1/100380 (<0.4)
At non-runs	0	<1/244881	17	1/183801 (<0.7)	5	1/460840 (<1.9)	6	1/556582 (<2.3)	16	1/76714 (<0.3)

^a Reported values for O_WT RT were taken from ref. [25].

^b Numbers between parentheses represent the RT's accuracy for each mutation type (given as fold-change of the error rate relative to the value obtained with O_WT RT).





THIS IS NOT THE VERSION OF RECORD - see doi:10.1042/BJ20101852

